J. Fluid Mech. (1977), *vol.* 82, *part* 4, *pp.* 659–671
Printed in Great Britain

The motion of two-dimensional vortex pairs in a ground effect

By STEVEN J. BARKER AND STEVEN C. CROW

School of Engineering and Applied Science, University of California, Los Angeles

(Received 1 July 1976 and in revised form 22 March 1977)

A new technique for generating a pair of line vortices in the laboratory has been developed. The mean flow of these vortices is highly two-dimensional, although most of the flow field is turbulent. This two-dimensionality permits the study of vortex motions in the absence of the Crow mutual induction instability and other three-dimensional effects. The vortices are generated in a water tank of dimensions $15 \times 122 \times 244$ cm. They propagate vertically and their axes span the 15 cm width of the tank. One wall of the tank is transparent, and the flow is visualized using fluorescein dye. High speed photography is used to study both the transition to turbulence during the vortex formation process and the interaction of the turbulent vortices with a simulated ground plane.

Transition occurs first in an annular region surrounding the core of each vortex, starting with a shear-layer instability on the rolled-up vortex sheet. The turbulent region then grows both radially inwards and radially outwards until the entire recirculation cell is turbulent. A 'relaminarization' of the vortex core appears to take place somewhat later.

The interaction of the vortex pair with the ground plane does not follow the predictions of potential-flow theory for line vortices. Although the total circulation is apparently conserved, the vortices remain at a larger distance from the ground than is expected and eventually 'rebound' or move away from the ground. Differences between a free-surface boundary condition and a smooth or rough ground plane are discussed. The ground-plane interaction is qualitatively very similar to that of aircraft trailing vortices observed in recent flight tests.

1. Introduction

The problems of aircraft wake turbulence have stimulated a number of recent measurements of vortex wake flows. Some of these measurements were made using full-scale aircraft to generate the vortices (Caiger & Gould 1971; Chevalier 1973). Other wake velocity measurements were made in wind tunnels (Mason & Marchman 1972) or in towing basins (Miller & Brown 1971; Lezius 1973). These measurements are subject to effects of probe interference: the presence of a physical velocity probe in the vortex wake causes the vortex to move away from the probe. There have been some recent measurements of wake vortex velocity profiles using laser anemometry, the results of which are not subject to probe interference (Baker *et al.* 1974; Orloff &

Grant 1973). These measurements compare reasonably well with the theoretical predictions of Saffman (1973).

All of these measurements of vortex wake velocities have been made in three-dimensional flow fields. Far downstream of the lifting surface, there are two significant three-dimensional effects that make such measurements difficult to interpret. Free-stream turbulence in the flow facility (or in the atmosphere) causes the vortices to be displaced randomly about their mean location in space. This 'vortex wandering' has the effect of making the vortices appear larger than normal in time-averaged velocity measurements. The effects of vortex wandering are discussed in detail in Baker *et al.* (1974). The second three-dimensional effect is the mutual induction instability, first described by Crow (1970). This instability causes the vortices to form 'kinks' along their length, which eventually result in a linking of the vortex pair into a series of vortex rings. It is nearly impossible to measure accurately in the laboratory the trajectories followed by vortex wakes in the presence of these two effects.

The goal of the present study is to determine the trajectories and decay rates of vortex pairs in a ground effect at moderately high Reynolds numbers. In view of the three-dimensional effects mentioned above, the best way to accomplish this is to create a two-dimensional vortex pair and study the flow field as a function of time. This will represent the flow in a plane transverse to a trailing vortex wake at a distance behind the aircraft of $x = Ut$. To obtain the highest possible Reynolds number on a laboratory scale, the experiment should be done in water. Water is also more suitable for making photographic measurements using flow-visualization techniques.

This experiment is not intended to simulate accurately the vortex wake behind a large aircraft. The ratio of core radius to vortex separation is higher in the experiment owing to the difference in Reynolds numbers. However, the experiment will provide us with an understanding of the qualitative nature of the interaction of finite core vortices with a ground plane.

2. Experimental apparatus

Several laboratory studies have been made of both laminar and turbulent vortex rings, such as that of Maxworthy (1974). A vortex ring can easily be generated in a water tank by ejecting a small amount of fluid through a sharp-edged circular orifice. The resulting rings are repeatable, and will propagate for many times their original diameter before dissipating. However, it is not as simple to generate a two-dimensional vortex pair which propagates for large distances from the generating mechanism. Some previous attempts at this have failed, and their failure was at first attributed to three-dimensional 'end-wall' effects.

A fundamental difference between a vortex ring and a vortex pair is in the size and shape of the recirculation cell. The recirculation cell for a vortex ring is a small toroid surrounding the axis of the vortex. For a two-dimensional pair, the recirculation cell is an oval enclosing both vortices whose shape is given by Lamb (1932):

$$0 = \frac{\Gamma}{2\pi}\left(\frac{x}{2s} + \log\frac{r_1}{r_2}\right). \qquad (1)$$

This equation relates to two vortices of circulation $\pm\Gamma$ with co-ordinates $(\pm s, 0)$. The radii r_1 and r_2 are the distances from each vortex to the point (x, y) on the cell boundary. The semi-axes of the recirculation cell are $2{\cdot}09s$ and $1{\cdot}73s$, so that the cell carries a much larger volume of fluid than that of a vortex ring of similar dimensions. Such a vortex pair will propagate vertically at a speed

$$dh/dt = \Gamma/4\pi s. \tag{2}$$

A device which generates a two-dimensional vortex pair must supply not only the necessary vorticity, but also the fluid to fill the recirculation cell. The 'puffing' technique used to form vortex rings does not satisfy the latter requirement. Therefore, attempts to create vortex pairs in this manner result in two vortices that are unable to propagate away from the generator. After the 'puff' has stopped, the vortices quickly draw together and dissipate.

Preliminary experiments in the present study demonstrated this difficulty, and led to the following technique for generating vortex pairs. To suppress completely the mutual induction instability and to avoid end-wall effects, it was decided to make the vortices 15 cm in length with an initial spacing of approximately 15 cm. The experimental tank was thus chosen to be 15 cm across, 122 cm deep and 244 cm long (figure 1, plate 1). These dimensions permit the vortex trajectories to be measured in a ground effect until they have reached a separation of eight times their original spacing. The vortex generating mechanism is located 24 cm from the bottom of the tank and is shown in figure 2 (plate 1). Two thin vertical plates span the 15 cm width of the tank and form a channel 12 cm wide and open at both top and bottom. When the experiment is ready to begin, a horizontal plate blocks this channel near its bottom (figure 2). This plate rapidly accelerates to a constant vertical velocity, pushing the fluid in the channel ahead of it. Fluid leaving the top end of the channel forms two vortex sheets beginning at the two sharpened ends of the channel walls. These vortex sheets immediately begin to roll up into a vortex pair.

After the horizontal plate has moved upwards a distance of 4 cm, it is abruptly retracted into the back wall of the tank. During this retraction motion the plate maintains its constant upward velocity. This 'disappearance' of the plate allows the vortex pair to leave the generator and propagate through the tank. If the plate is not retracted, the vortices immediately draw together and dissipate. The retraction allows the upwash in the vertical channel to decay slowly rather than abruptly, thus providing the necessary fluid for the vortex recirculation cell.

The mechanical apparatus for executing the somewhat complex motion of the horizontal plate is located in a flooded box on the outside of the back wall of the tank. The vertical motion is driven by a constant-speed a.c. motor which pulls a connecting rod through a seal in the flooded box. After the horizontal plate has moved upwards 4 cm, a trip level in the flooded box actuates a spring-loaded retraction mechanism. The plate retraction takes place in about 0·1 s.

The front wall of the tank is made of 5 cm thick Plexiglas to permit flow visualization. For high speed motion pictures, the best results are obtained using fluorescein dye against a flat black background. The dye is illuminated from above by four 600 W quartz lamps. (Heating of the water by these lamps was carefully avoided.) Before the experiment begins, the vortex generator is partially filled with the dye, which then provides excellent contrast during the vortex motion. Motion pictures are taken at speeds of 64 and 200 frames/s and then projected on sheets of paper at speeds of between 1 and 24 frames/s. The trajectories of the two vortex cores are traced on the paper, and time marks are added.

The vortices propagate upwards rather than downwards in this experiment to facilitate the study of the ground-plane interaction. With this geometry we can observe three different boundary conditions on the ground plane. We investigate a free-surface boundary condition (zero stress), a rigid smooth ground plane and a rigid rough ground plane. Furthermore, it is more practical to vary the distance between the vortex generator and the ground plane by changing the water depth than by moving the generator itself.

3. Results

The discussion of results will be divided into two parts: vortex instability and transition, and vortex-trajectory measurements.

Instability and transition

There has been much speculation about whether the flow in the cores of a vortex wake far downstream of the lifting body is largely laminar or turbulent. According to the Rayleigh stability criterion, any vortex will be stable as long as the absolute value of the circulation increases monotonically with radius. Most vortex velocity distributions of aerodynamic interest (figure 3) are stable by this criterion. However, the Rayleigh criterion applies only to axisymmetric disturbances of the form

$$u' = f(r) \exp [i(kz - \omega_r t)] \exp (\omega_i t), \tag{3}$$

where z and r are co-ordinates parallel to and perpendicular to the vortex axis. This criterion says nothing about the more general 'helical waves', of the form

$$u' = f(r) \exp [i(kz + m\theta - \omega_r t)] \exp (\omega_i t). \tag{4}$$

Kelvin analysed the special case of the Rankine vortex (figure 3) and found it to be stable to all disturbances, including helical waves. However, the Rankine vortex is a special case involving an abrupt change from solid-body rotation in the core to a potential-vortex outer region. Crow (1975) has shown by means of a global energy equation that helical disturbances can extract energy from the mean flow in the transition region between the core and potential vortex. In particular, the cylindrical vortex sheet (figure 3) was analysed and shown to be unstable to helical disturbances of wavenumber m greater than or equal to 3. From these considerations we might expect two-dimensional vortices to be unstable in an annular region surrounding the core.

The initial velocity profile created in this experiment does not correspond to any of the axisymmetric profiles of figure 3. As the horizontal plate moves upwards, two vortex sheets are generated and immediately begin to roll up. The velocity profile of the early vortex thus has a number of steps in it, the circulation increasing discontinuously at each step. Similar steps will occur in the near field of the aircraft trailing vortex wake, but in this case they arise from the roll-up at the two ends of a single horizontal vortex sheet.

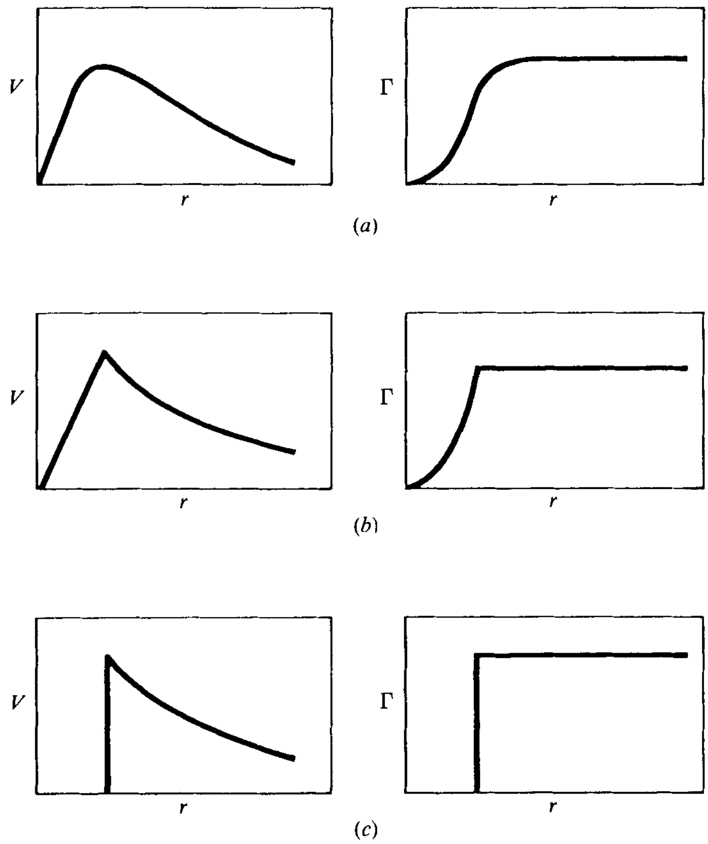

FIGURE 3. Model vortex velocity distributions. (*a*) Gaussian vortex. (*b*) Rankine vortex. (*c*) Cylindrical vortex sheet.

Figures 4(*a*) and (*b*) (plate 2) are flow-visualization photographs of a vortex pair during the roll-up process. The vortex circulation, as determined from the propagation velocity (2) of the pair, is 240 cm^2/s. The vortex Reynolds number, defined as Γ/ν, is 25000. Relatively low speed vortices were used in the studies of roll-up and initial instability. We see that an amplified disturbance occurs on the vortex sheet throughout the roll-up. This instability is similar in appearance to the Kelvin–Helmholtz instability of a free shear layer, such as that observed by Brown & Roshko (1974). The eddies seen by Brown & Roshko occur even at very high Reynolds numbers in a fully turbulent flow. The wavelength of these eddies is proportional to the 'vorticity thickness' of the free shear layer, defined by

$$\delta_\omega = \frac{1}{|\omega|_m}\int_{-\infty}^{\infty} |\omega| dy. \tag{5}$$

Brown & Roshko found the measured wavelength of the eddies to equal $2{\cdot}9\delta_\omega$.

The flow in the present experiment is time dependent and the length used to normalize the eddy wavelength must be a function of time. Since the wavelike instability was observed only for times less than about 2 s, the boundary-layer thickness on the inside walls of the channel plates can be crudely approximated by $\delta = 4(\nu t)^{\frac{1}{2}}$. Movies of the initial roll-up process were taken at 200 frames/s and analysed one frame at a time to determine the eddy wavelength λ as a function of time. When λ is plotted *vs.* $4(\nu t)^{\frac{1}{2}}$, the slope of the best-fit straight line is 2·6. This is in rather good agreement with the Brown & Roshko value of 2·9 considering the gross differences between the two experiments.

The boundary layer at the ends of the two channel plates is thin and laminar. To thicken this boundary layer and observe the effect upon the initial instability sawtooth vorticity generators were installed on the ends of the plates. The teeth were spaced 0·6 cm apart and protruded 0·3 cm perpendicular to the channel walls. Two significant differences were observed in the movies with the sawteeth installed. The instability waves were not seen at all until more than 1 s after the motion had begun. Without the teeth, these waves can be seen as early as 0·2 s. In addition, the wavelength of the instability was almost twice as large with the sawteeth as without. When λ is plotted *vs.* $4(\nu t)^{\frac{1}{2}}$ as before, the slope of the straight line becomes 4·7. These two changes are qualitatively what we should expect for the shear-layer instability.

As the roll-up proceeds further, the initial instability wave grows to an amplitude of approximately one-tenth of the spacing between the vortices (figure 4*b*). At this point a rather sudden transition to turbulence occurs, and within another 0·2 s the vortices have the appearance shown in figure 5 (plate 3). The motion pictures show that transition begins in the annular region of the instability waves and progresses both radially inwards and radially outwards. The flow in the vortex recirculation cell remains fully turbulent until the vortices have dissipated, except for a small region near the centre of each vortex. This inner region appears to remain laminar and grow slowly in radius during the evolution of the vortex. Although it can be seen in figure 5, the laminar region cannot be distinguished so well in a still photograph as in the movies.

The fact that transition begins in an annular region is in agreement with the prediction of the stability calculation discussed above. The laminar appearance of the core region of the vortex can be correlated with observations of aircraft trailing vortices. Aircraft vortices are visualized by vapour condensation in the low pressure vortex cores. Thus the 'flow visualization' covers only the inner core region, where the flow may indeed by laminar. The turbulent region surrounding the core is not visualized, hence observers may be tempted to conclude that the vortices are predominately laminar. In a recent study of aircraft vortices near the ground, smoke was injected into both the core and the outer region (Tombach, Crow & Bate 1975). In this case, the outer region was clearly turbulent, as in the present experiment.

At this point, it is appropriate to discuss the two-dimensional nature of the mean flow in the experiment. Since the vortex axes are bounded by walls at both ends, the end-wall boundary layers are possible sources of three-dimensional effects. The pressure of the mean flow falls towards the centre of each vortex, which tends to produce a secondary flow in the end-wall boundary layers. This secondary flow would be radially inward, and could thus cause fluid from the boundary layer to be 'pumped' into the core of each vortex. This pumping into the core would reduce the total circulation of the vortex, increase the thickness of the core, and also produce an axial mean flow along the vortex lines inwards from the walls towards the centre.

Three independent observations show that this boundary-layer effect is insignificant.

(i) Dyed fluid that is initially on or near the end walls is not sucked into the core of the vortex as it passes by.

(ii) Small air bubbles can be injected into the vortex cores and will remain there owing to the pressure minimum. They distribute themselves uniformly along the vortex axes and show no mean axial motion towards the centre of the length. They do move randomly back and forth along the axes in a manner very similar to small balloons trapped in the cores of aircraft vortices (Tombach *et al.* 1975).

(iii) The total circulation does not change while the vortices are out of the ground effect: their separation and propagation velocity remain constant.

Simple dimensional analysis also suggests that boundary-layer effects should not be important. The vortices are not stationary with respect to the end walls in the experiment, so that the wall boundary layers will not grow to a steady-state thickness as an Ekman layer would. The boundary-layer thickness is thus proportional to $(\nu t)^{\frac{1}{2}}$, where t is the time required for the recirculation cell to pass over a fixed point on the wall. This time is approximately 0·5 s, so that the boundary-layer thickness is of the order of 0·07 cm.

Vortex trajectories in ground effect

The behaviour of aircraft wake vortices in a ground effect is extremely important in determining the possible dangers of vortices left near the runway by arriving and departing aircraft. If the wake vortices behaved like potential line vortices, their trajectories could be predicted quite readily. Lamb (1932) gives the solution to the problem of a pair of line vortices interacting with an image pair of opposite sign. The x axis becomes the 'ground plane' and the vortices propagate at velocities

$$\dot{s} = \frac{\Gamma}{2\pi}\frac{s^2}{hr^2}, \quad \dot{h} = \frac{\Gamma}{2\pi}\frac{h^2}{sr^2}. \tag{6}$$

Here s and h are the x and y co-ordinates of the vortex in the upper right quadrant and $r^2 = s^2+h^2$. The trajectories can be written in the form

$$s_0^2(s^2+h^2) = s^2h^2, \tag{7}$$

where s_0 is the half-spacing of the vortices when they are far above the ground. After the vortices have spread apart some distance in the ground effect, they should approach a distance above the ground of s_0.

For the present trajectory measurements, two different water depths were used in the tank. Since the core radius will grow with the time from generation, the different depths will demonstrate the effects of the core radius upon the ground-effect trajectory. Two values of the vortex circulation were also used to check for dependence upon the Reynolds number. The circulations, as determined by the propagation velocity $\dot{h}$ far from the ground plane, were 250 and 750 cm²/s. The corresponding vortex Reynolds numbers Γ/ν were 25000 and 75000.

Since it was also desired to determine the effect of the ground-plane boundary condition upon the trajectory, three different simulated ground planes were used. One of these was a free surface, with the boundary conditions $\partial u/\partial y = 0$ and $v = 0$. The second ground plane was a horizontal sheet of smooth Plexiglas immersed in the

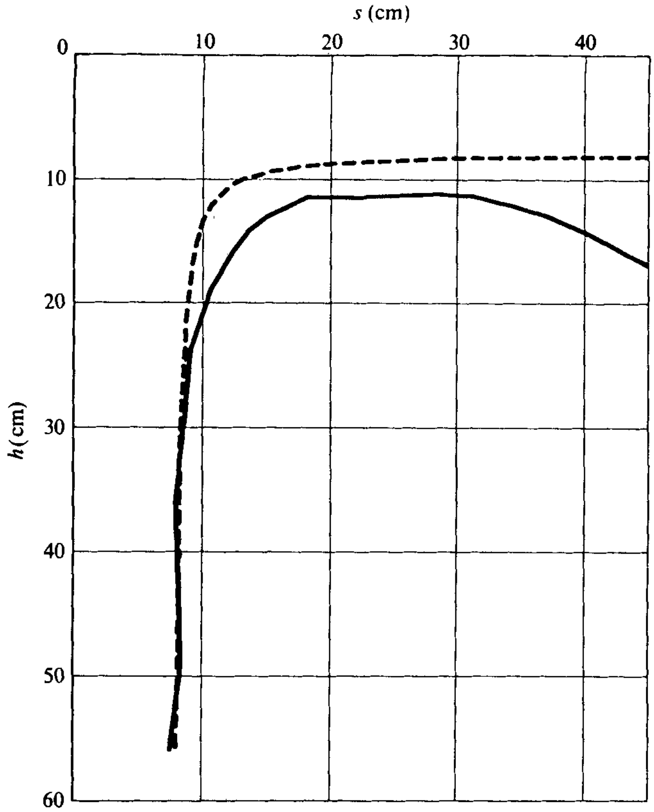

FIGURE 6. Vortex trajectory (solid curve) compared with line-vortex theory (dashed curve).

water. The third was a 'rough ground plane', a sheet of Plexiglas with grooves cut across the 15 cm width. It was expected that the boundary layers on the two rigid planes would gradually reduce the circulation of the vortices in the ground effect.

Figure 6 shows an experimental vortex trajectory compared with the line-vortex trajectory (7). The experimental trajectory is the average of the trajectories of the two vortices of the pair. The initial circulation of each vortex is 750 cm^2/s. The ground plane in this case is the free surface. The vortices follow the line-vortex trajectory closely for the first 30 cm of vertical motion, or until they are 25 cm below the surface. At this point they begin to spread apart sooner than the line-vortex prediction and they remain further below the surface as they spread. When the half-separation of the vortices reaches about 30 cm, they suddenly begin to move away from the surface. This unexpected motion away from the surface, which we shall call 'rebounding', is very repeatable and always occurs simultaneously in both vortices of the pair. It is not caused by the imaging effect of the side walls of the tank, since these walls are 90 cm away from the vortices when the rebounding begins. The downward vertical velocity induced by the side-wall image pair has been calculated and is negligible.

In recent flight test measurements of vortex wake trajectories in a ground effect, Tombach *et al.* (1975) observed that a 'rising' of the vortices occurred occasionally after they had levelled out parallel to the ground. This occurred most often when the

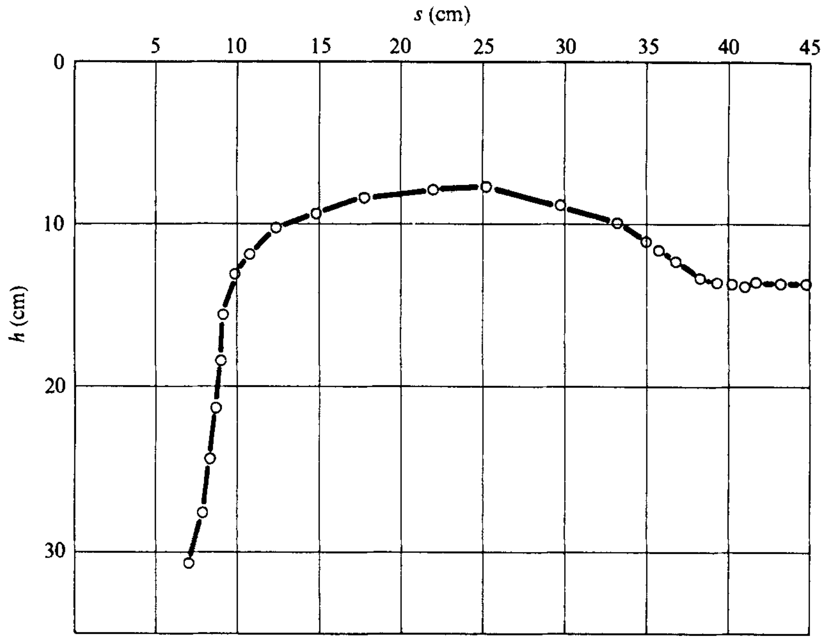

FIGURE 7. Vortex trajectory with generator near surface.

aircraft was flying very near to the ground. Current numerical computations of finite core vortices interacting with a ground plane have produced similar behaviour. The present authors have not found any other examples of a rebounding effect in the experimental literature. However, there is very little quantitative data available on full-scale wake vortex trajectories extending far enough into a ground effect to see the rebounding.

Figure 7 shows a vortex trajectory measured under the same conditions as in figure 6, except that the distance from the generator to the surface is half as great. There are two distinct differences between these trajectories. The pair generated closer to the surface reaches a depth of 8 cm before rebounding begins, whereas the other pair reached a depth of only 11 cm. When the near-surface vortex pair begins to rebound, it does so more severely and then levels off again at a distance of about 14 cm from the surface. This result is also in qualitative agreement with the flight test data. All of these results can be attributed to the effects of finite core radius, which will be discussed below.

Figure 8 shows the co-ordinates of the vortex pair of figure 7 plotted as functions of time. The slope of the *s vs. t* curve changes suddenly during the rebounding period, at about 8 s. In view of this, it should also be of interest to plot the 'apparent circulation' of the vortex *vs.* time. We define the apparent circulation to be the value of Γ determined from the line-vortex trajectory formula

$$\Gamma = 4\pi q \frac{sh(s^2+h^2)}{(s^6+h^6)^{\frac{1}{2}}}. \tag{8}$$

Here q is the propagation speed of the vortex $(\dot{s}^2+\dot{h}^2)^{\frac{1}{2}}$. This formula does not give the true circulation of the vortex since the exact shape of the vorticity-containing

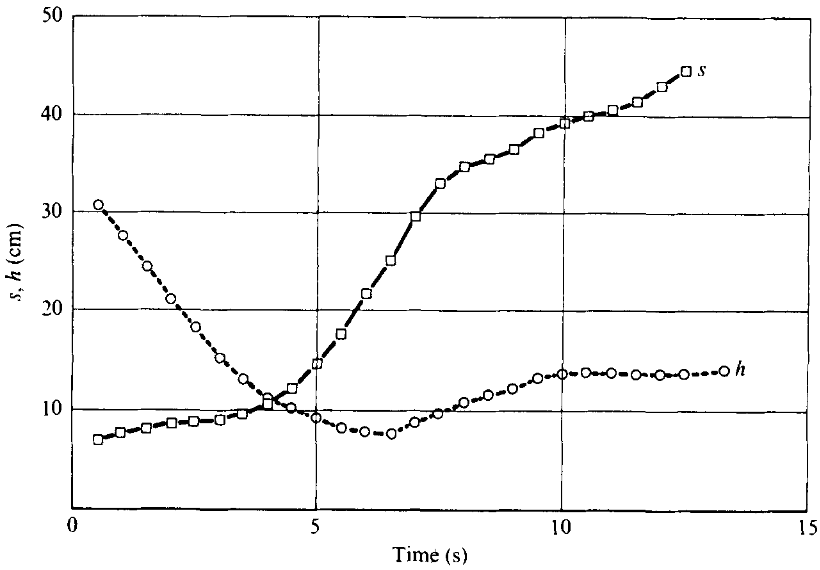

FIGURE 8. Vortex co-ordinates *vs.* time.

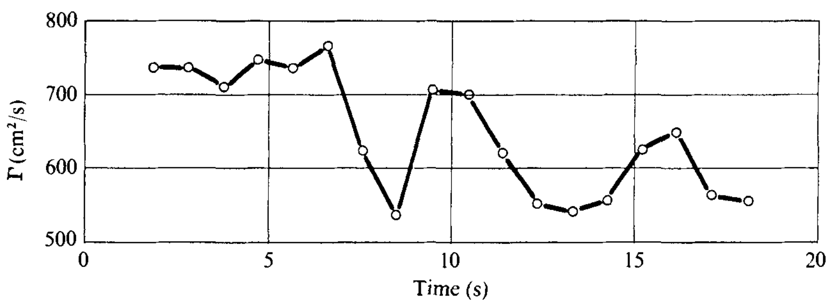

FIGURE 9. Apparent circulation *vs.* time.

core has not been accounted for. A typical plot of apparent circulation *vs.* time is shown in figure 9. The circulation remains nearly constant for the first six seconds, during which the pair is propagating vertically at constant velocity and constant separation. The circulation then undergoes a series of oscillations which are repeatable both in amplitude and frequency. These oscillations occur during the interaction with the ground plane and the rebounding process.

Trajectories can also be plotted in a dimensionless form, and then compared with the flight test experiments. In figure 10, we have plotted the normalized half-separation s/s_0 as a function of the normalized time $\Gamma_0 t/s_0^2$, for both the present experiment and the flight test data of Tombach *et al.* The flight data are for an Aero-Commander 560A twin-engine aircraft flying at 8 m above the ground. The

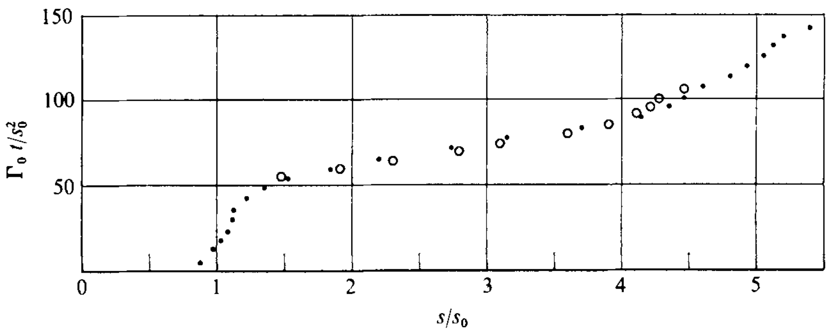

FIGURE 10. Normalized vortex trajectory (solid circles) compared with flight test data (open circles).

initial half-separation s_0 was 5 m. The apparent circulation Γ_0 for the flight data was calculated from the horizontal propagation speed of the vortices as they spread apart in the ground effect. The time origin of the flight test data has been shifted such that the first point coincides with the first point of the laboratory data. The agreement between these normalized trajectories is striking.

The upward curvature of the data curve in figure 10, beginning at an s/s_0 of about 4, indicates a slowing down of the rate of separation. This slowing down is coincident with the occurrence of rebounding, and must take place if the total circulation is conserved during the rebounding process. If this phenomenon is indeed a result of a finite core radius, we should attempt to determine the core radii in the experiment and compare these with typical aircraft values. Spreiter & Sacks (1951) have analysed the roll-up of the vortex sheet behind an elliptically loaded wing, and found that the core radius of the fully rolled-up vortex is 0·2 times the half-spacing of the vortices. There is no easy way to calculate the core radius for the present experiment, but it can be determined at least approximately from studies of the high speed movies of the roll-up process. These movies indicate that the ratio of core radius to half-spacing in the experiment ranges from 0·3 to 0·4. Thus the core radius in the experiment is at least 50 % greater than that expected for an aircraft trailing vortex from a high aspect ratio wing. The effects of finite core radius upon the vortex trajectory may then be somewhat exaggerated in the experiment. However, the comparison with full-scale results shown here indicates that the effects are at least qualitatively similar.

The presence of either of the rigid ground planes has little effect upon the gross properties of the vortex motion. The trajectories are nearly the same and the oscillations in apparent circulation occur at the same frequency. However, the rigid planes do cause a gradual loss of apparent circulation as the vortices spread out in the ground effect. The loss amounts to about 20 % for the smooth plane and slightly more for the rough plane. There is no obvious dependence of this loss upon Reynolds number in the data.

4. Conclusions

The most unexpected result of this experiment is the 'rebounding' effect, which consistently takes place after the vortices have spread in a ground effect to about four times their original separation. The qualitative agreement with the flight test trajectories shows that this effect is not an artifact of the experiment. The explanation of the rebounding almost certainly lies in the effects of finite vortex core radius. The dynamics of a vortex pair of finite core radius interacting with an image plane are complex, but it is intuitively apparent that a circular core will be deformed into a non-circular shape when it nears the surface. In fact, the eccentricity of the vortices can be seen in figure 11 (plate 4), which shows a dyed vortex pair close to the surface. Once a vortex core has been deformed, it would be expected to become unsteady in shape and vorticity distribution. An elliptical vortex core might have a tendency to rotate as it moved along the image plane. This would lead to changes in both the distance of the vortex centre from the surface and the propagation velocity of the centre. Such an effect could explain both the rebounding and the periodic oscillation of the apparent circulation.

If we model the vortex core as an ellipse in solid-body rotation, we can predict the period of the oscillations. The result of this crude model is a period of 3 s, which is in fairly good agreement with the data plotted in figure 9. The eccentricity of the vortex cores has also been predicted by a numerical simulation study currently in progress. In fact, the core shapes predicted by the numerical simulation are almost exactly those seen in the experiment.

In future studies we shall measure fluid velocities in the vortex flow field and determine more precisely the dimensions of the vortex cores. The dependence of the trajectories upon the exact vorticity distribution can then be determined. The agreement between the present normalized trajectory plot and that of the flight tests (figure 10) may indicate that the ratio of core radius to initial vortex spacing is roughly the same for the shallow-generated vortices as in the flight tests. The trajectories of vortices generated at a greater depth do not agree so well with the flight tests, presumably because these vortices have a larger ratio of core radius to separation when they reach the surface. Previous numerical studies have shown that a large core radius can lead to instabilities in which the two vortices tear each other apart. The movies of the present experiment show a core instability taking place after the rebounding process, which might result from this mechanism.

This experimental technique has been shown to be extremely useful in simulating large-scale two-dimensional vortex dynamics in the laboratory. Effects of finite core radius can be observed in the laboratory and are also found in flight test data. These effects had not been expected before the experiment. As a practical consideration for the abatement of aircraft wake turbulence near an airport runway, any feasible method of increasing the vortex core radius should be investigated. The laboratory experiment will now be used to study the effects of stable fluid stratification upon the vortex dynamics.

The authors wish to acknowledge the support of the Transportation Systems Center of the Department of Transportation, and Aerovironment, Inc., for their sponsorship of this research.

REFERENCES

BAKER, G. R., BARKER, S. J., BOFAH, K. K. & SAFFMAN, P. G. 1974 *J. Fluid Mech.* **65**, 325.

BROWN, G. L. & ROSHKO, A. 1974 *J. Fluid Mech.* **64**, 775.

CAIGER, B. & GOULD, D. 1971 An analysis of flight measurements in the wake of a jet transport aircraft. In *Aircraft Wake Turbulence and its Detection* (ed. Olsen), p. 125. Plenum.

CHEVALIER, H. 1973 *J. Aircraft* **10**, 14.

CROW, S. C. 1970 *A.I.A.A. J.* **8**, 2172.

CROW, S. C. 1975 The stability of vortex cores. *Poseidon Res. Note* no. 4.

LAMB, H. 1932 *Hydrodynamics*, 6th edn, p. 223. Dover.

LEZIUS, D. 1973 Study of the far wake vortex field generated by a rectangular airfoil in a water tank. *A.I.A.A. Paper*, no. 73–682.

MASON, H. & MARCHMAN, J. 1972 The farfield structure of aircraft wake turbulence. *A.I.A.A. Paper*, no. 72–40.

MAXWORTHY, T. 1974 *J. Fluid Mech.* **64**, 227.

MILLER, E. & BROWN, C. 1971 An experimental study of trailing vortex wakes using a large towing tank. *Hydronautics Tech. Rep.* no. 7105–1.

ORLOFF, K. & GRANT, G. 1973 The application of a scanning laser-Doppler velocimeter to trailing vortex definition and alleviation. *A.I.A.A. Paper*, no. 73–680.

SAFFMAN, P. G. 1973 *Phys. Fluids* **16**, 1181.

SPREITER, J. R. & SACKS, A. H. 1951 *J. Aero. Sci.* **18**, 21.

TOMBACH, I. H., CROW, S. C. & BATE, E. R. 1975 Investigation of vortex wake stability near the ground. *Aerovironment, Inc., Final Rep.* AV FR 538.